Vietnam Journal of Mechanics, VAST, Vol. 43, No. 3 (2021), pp. 237 – 252
DOI: https://doi.org/10.15625/0866-7136/15533

PROPAGATION OF WAVES IN AN INCOMPRESSIBLE ROTATING TRANSVERSELY ISOTROPIC NONLOCAL ELASTIC SOLID

Baljeet Singh[1,*]
[1]*Department of Mathematics, Post Graduate Government College, Sector-11, Chandigarh 160011, India*
[*]E-mail: bsinghgc11@gmail.com

Received: 22 September 2020 / Published online: 30 July 2021

Abstract. In this paper, the nonlocal elasticity theory is applied to study the propagation of plane wave and Rayleigh-type surface wave in an incompressible, rotating and transversely isotropic material. The governing equations of motion for an incompressible, rotating, transversely isotropic and nonlocal elastic medium are specialized for a plane. The medium is assumed rotating about an axis perpendicular to the plane. The transverse isotropy axis is taken perpendicular to the surface. The specialized governing equations are first applied to derive a velocity equation for homogeneous plane wave. The specialized governing equations along with traction free boundary conditions are also applied to derive the secular equation governing the wave speed of Rayleigh wave. The speeds of plane wave and Rayleigh wave are computed and illustrated graphically to observe the effects of nonlocality, rotation, anisotropy, frequency and propagation direction. It is noticed from the theory and numerical results that the speeds of both plane wave and Rayleigh wave decrease sharply with an increase in nonlocal parameter or rotation parameter. The speeds of plane wave and Rayleigh wave increase logarithmically with anisotropy material parameter. The feasible ranges of nonlocality, rotation or anisotropy parameters for the existence of plane wave or Rayleigh surface wave are determined for a given wave speed when the values of other parameters are fixed.

Keywords: nonlocal elasticity, transverse isotropy, rotation, plane waves, Rayleigh wave.

1. INTRODUCTION

In recent years, the materials and structures have been considered on nano-scale to meet the requirement of various acoustic devices to have greater sensitivity and storage within smaller structure. The classical elasticity is unable to predict properly the nature of such nano-scale materials. For instance, the behaviour of materials with fractures, dislocation, cracks, singularities and discontinuities can not be treated completely by the local elasticity theory [1, 2]. Taking material microstructure into account, Eringen [3, 4]

proposed a nonlocal differential model where the stress at a given reference point is considered as a function of the strain of all points and included a material parameter representing the internal length scale into the stress–strain relation.

Peddieson et al. [5] pioneered the applications of nonlocal continuum mechanics to analyze the size-effects in micro and nanoscale structures. They applied the nonlocal elasticity to study the bending of micro and nanoscale beams and found that the significance of the size-effects for nano-sized structures largely depends on the value of the nonlocal parameter which captures the small scale effect on the response of nanostructures. For verification of nonlocal continuum models, an accurate estimate of small-scale or nonlocal parameter is required. A theoretical procedure to determine the small scale parameter in nonlocal elasticity is not derived yet. Eringen [3, 4] proposed the small scale parameter as 0.31 nm and 0.39 nm in his studies on plane and Rayleigh surface waves, respectively, by comparing the dispersion curves via lattice dynamics and nonlocal continuum mechanics. Due to potential applications of carbon nanotubes and graphene sheets in designs of new sensors, gas detection and composite materials, various models of based on these nanomaterials were explored. For example, Sudak [6], Zhang et al. [7], Sears and Batra [8], Wang [9], Wang and Hu [10], Xie et al. [11], Wang and Wang [12], Tounsi, et al. [13], Arash and Ansari [14], Liang and Han [15], Ghavanloo and Fazelzadeh [16], Hemadi, et al. [17], Tuna and Kirca [18] and various other researchers contributed towards the estimation of the small scale parameters for carbon nanotubes models. For graphene sheets models, various researchers including Ansari et al. [19], Huang et al. [20], Madani et al. [21] and Jalali [22] estimated the nonlocal parameter using different numerical modeling and simulations. Arash and Wang [23] reviewed the possible applications of the nonlocal continuum theory for carbon nanotubes and graphene sheets models. According to the predictions of above studies, the crystal structure in lattice dynamics, boundary conditions, vibrational mode number and mechanical model under investigation are the deciding factors to obtain an optimum value of nonlocal parameter.

The nonlocal continuum theory was applied in various wave propagation problems. Based on the nonlocal elasticity, Eringen [3, 4] analyzed the bulk and surface waves and found that the elastic waves are dispersive in a nonlocal linearly elastic medium. The nonlocal elasticity was also employed in some other wave propagation problems by various researchers including Narasimhan and McCay [24], Inan and Eringen [25], Ke et al. [26], Sapora et al. [27], Roy et al. [28], Tong et al. [29], Singh et al. [30], Kaur et al. [31], Ma et al. [32], Yan et al. [33], Tung [34], Singh [35] and references therein.

Motivated by the requirements of seismology including prediction of earthquakes, a time-harmonic surface wave was investigated by Lord Rayleigh [36] on a traction free boundary of a linearly elastic isotropic half-space. Different geometrical configurations and physical constants of a material affect the wave attributes. Various important acoustic sensors have been investigated due to these geometrical and physical influences of materials on wave features (White [37], Tiersten et al. [38, 39], Wren and Burdess [40]). Schoenberg and Censor [41] discovered the rotational effects on bulk and surface waves

in an elastic solid. Auriault [42] also investigated bulk wave speeds in an isotropic linearly elastic solid with rotational effects. Clarke and Burdess [43, 44] recognized a device for possible use in rotation sensing and analysed the Rayleigh waves over a rotating isotropic half-plane. Some other linear rotating anisotropic model were investigated for wave features by various researchers including Fang et al. [45], Destrade [46, 47], Ting [48], Ogden and Singh [49], Vinh and Hue [50], Singh and Kaur [51, 52] and references therein.

The secular equation of the Rayleigh wave is very crucial for computing of wave speed when material parameters are given. Also, the material parameters may also be accurately estimated for a given wave speed. Rayleigh-type surface waves have been applied in various scientific areas including acoustics, geophysics and seismology. To the best of author's knowledge, there is no investigation available in the literature which have considered the propagation of plane waves and Rayleigh-type surface waves in a rotating and transversely isotropic half-space of a linearly incompressible nonlocal elastic material. The presence of nonlocality and rotation parameters adds more complexity in an incompressible transversely isotropic model. Therefore, the main focus of this study is to illustrate the impact of nonlocal, rotation and anisotropy parameters on the speeds of both plane and Rayleigh waves. In Section 2, the equations governing the nonlocal elasticity of a linear, homogeneous, rotating, transversely isotropic and incompressible material are specialized for a plane. In Sections 3 and 4, a velocity equation of homogeneous plane wave and a secular equation governing the speed of Rayleigh wave are derived by using traditional techniques. In Section 5, some limiting cases of the Rayleigh wave equation are discussed. The speed dependence of both plane and Rayleigh waves on rotation, nonlocality and anisotropy (transverse isotropy) is illustrated graphically in Section 6. The findings based on the theory and numerical simulation are summarized in the last section.

2. GOVERNING EQUATIONS

We introduce a Cartesian coordinates system (x_1, x_2, x_3). A transversely isotropic elastic half-space is considered with x_1-axis along the surface and the x_3-axis normal into the half-space. In a transversely isotropic medium, the isotropy plane is taken perpendicular to the x_3-axis. The present problem is confined to (x_1, x_3) plane with displacement components u_1 and u_3 in x_1- and x_3-directions, respectively. The half-space is assumed as rotating with an angular rate Ω about x_2-axis as shown in Fig. 1. According to Eringen [1, 3, 4] and Schoenberg and Censor [41], the two-dimensional governing equations for an incompressible, linear, homogeneous, rotating, transversely isotropic

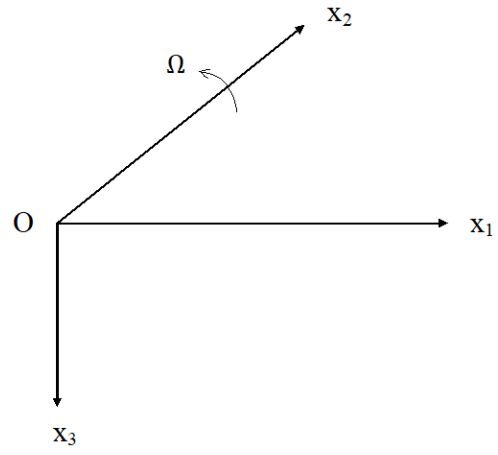

Fig. 1. The configuration of the model

and nonlocal elastic solid in (x_1, x_3) plane are expressed as

$$\frac{\partial \tau_{11}}{\partial x_1} + \frac{\partial \tau_{13}}{\partial x_3} = \rho\Big(\frac{\partial^2 u_1}{\partial t^2} - \Omega^2 u_1 + 2\Omega\frac{\partial u_3}{\partial t}\Big), \tag{1}$$

$$\frac{\partial \tau_{13}}{\partial x_1} + \frac{\partial \tau_{33}}{\partial x_3} = \rho\Big(\frac{\partial^2 u_3}{\partial t^2} - \Omega^2 u_3 - 2\Omega\frac{\partial u_1}{\partial t}\Big), \tag{2}$$

where

$$\begin{aligned}(1-\epsilon^2\nabla^2)\tau_{11} &= -P + B_{11}\frac{\partial u_1}{\partial x_1} + B_{13}\frac{\partial u_3}{\partial x_3},\\ (1-\epsilon^2\nabla^2)\tau_{33} &= -P + B_{13}\frac{\partial u_1}{\partial x_1} + B_{33}\frac{\partial u_3}{\partial x_3},\\ (1-\epsilon^2\nabla^2)\tau_{13} &= B_{44}\Big(\frac{\partial u_1}{\partial x_3} + \frac{\partial u_3}{\partial x_1}\Big),\end{aligned} \tag{3}$$

and ∇^2 is Laplacian operator and is given by $\nabla^2 = (\partial/\partial x_1)^2 + (\partial/\partial x_3)^2$, ϵ is a nonlocality parameter $(\epsilon = \epsilon_0 h/L)$ which captures the small scale effect in nano-size structures, ϵ_0 is a material coefficient, h an internal characteristic length (granular size, lattice parameter, distance between $C-C$ bonds), L is an external characteristics length (wave length, crack length), ρ is the mass density of material, $P = P(x_1, x_2, t)$ is the hydrostatic pressure due to incompressibility and B_{11}, B_{13}, B_{33} and B_{44} are the positive elastic constants which satisfy inequalities $B_{11} + B_{33} - 2B_{13} > 0$.

The condition of incompressibility is written as

$$\frac{\partial u_1}{\partial x_1} + \frac{\partial u_3}{\partial x_3} = 0. \tag{4}$$

From Eq. (4), there exists a scalar function $\psi(x_1,\ x_2,\ t)$ such that

$$u_1 = \frac{\partial \psi}{\partial x_3},\ u_3 = -\frac{\partial \psi}{\partial x_1}. \tag{5}$$

Using Eqs. (3) and (5) in Eqs. (1) and (2) and eliminating P, an equation in scalar ψ is derived as

$$\begin{aligned}&B_{44}\frac{\partial^4 \psi}{\partial x_1^4} + (B_{11} - 2B_{13} + B_{33} - 2B_{44})\frac{\partial^4 \psi}{\partial x_1^2 \partial x_3^2} + B_{44}\frac{\partial^4 \psi}{\partial x_3^4}\\ &= \rho(1-\epsilon^2\nabla^2)\Big[\frac{\partial^4 \psi}{\partial x_1^2 \partial t^2} + \frac{\partial^4 \psi}{\partial x_3^2 \partial t^2} - \Omega^2\Big(\frac{\partial^2 \psi}{\partial x_1^2} + \frac{\partial^2 \psi}{\partial x_3^2}\Big)\Big].\end{aligned} \tag{6}$$

3. PLANE WAVES

For plane wave propagation in an incompressible, rotating, transversely isotropic and nonlocal elastic material, the solution ψ of Eq. (6) can be expressed as

$$\psi = g\Big(ik(s_1 x_1 + s_3 x_3 - vt)\Big), \tag{7}$$

where v is the wave speed, k is the wave number, t is time and g is function of the specified argument and s_1, s_3 with $s_2 = 0$, are components of a unit vector **s** along the co-ordinate

axes. Here $(s_1, s_3) = (\cos\theta, \sin\theta)$ are the direction cosines of propagation direction in (x_1, x_3) plane such that

$$s_1{}^2 + s_3{}^2 = 1, \tag{8}$$

where θ is the angle of propagation measured from normal to the surface.

Substituting (7) and (8) in Eq. (6), a velocity equation in non-dimensional wave speed of homogeneous plane wave is derived as

$$V^2 = \frac{1 + (\delta - 4)s_1{}^2 s_3{}^2}{\Omega^*} - e, \tag{9}$$

where $V^2 = \rho v^2 / B_{44}$, $\delta = (B_{11} + B_{33} - 2B_{13})/B_{44}$, $e = \rho\omega^2\epsilon^2/B_{44}$, $\Omega^* = 1 + \Omega_0^2$, $\Omega_0 = \Omega/\omega$, $\omega = kv$ is the wave circular frequency. For real and positive V, the following necessary condition is required

$$e < \frac{1 + (\delta - 4)s_1{}^2 s_3{}^2}{\Omega^*}. \tag{10}$$

The possible ranges of circular frequency ω or nonlocal parameter ϵ or rotation parameter Ω or anisotropy parameter δ for plane wave propagation in the considered model can be determined by using inequality (10) when other parameters are fixed. The non-dimensional nonlocality parameter e in Eq. (9) is directly proportional to dimensional nonlocal parameter ϵ and circular frequency ω. Therefore, the speed decreases when ϵ or ω or both increases. From Eq. (9), it can also be predicted that the speed decreases by increasing the rotation parameter Ω. In limit of low frequency $(\omega \to 0)$, the non-dimensional parameter e tends to zero and the rotation parameter Ω^* tends to infinity. Then according to Eq. (9), the speed of plane wave tends to zero. In limit of high frequency $(\omega \to \infty)$, it is also seen from Eq. (9) that the speed of plane wave decreases first as ω increases and tends to zero at a cutoff frequency. Beyond this critical value of frequency, the speed reduces to a purely imaginary value.

In absence of nonlocality parameter $(\epsilon \to 0)$, the non-dimensional parameter e tends to zero and the velocity equation (9) can be reduced as

$$V = \sqrt{\frac{1 + (\delta - 4)s_1{}^2 s_3{}^2}{\Omega^*}}. \tag{11}$$

4. RAYLEIGH WAVE

Now, we consider a Rayleigh-type wave propagating with positive speed c and positive wave number k along the x_1-axis and decaying with the x_3-axis, that is

$$u_i \to 0 \ (i = 1, 3) \text{ as } x_3 \to +\infty. \tag{12}$$

The following traction free boundary conditions are applied on the surface $x_3 = 0$

$$\tau_{13} = 0, \ \tau_{33} = 0 \text{ at } x_3 = 0. \tag{13}$$

With the use of Eqs. (1), (3) and (5), the boundary conditions (13) are expressed in terms scalar function ψ as

$$B_{44}\Big(\frac{\partial^2\psi}{\partial x_3^2}-\frac{\partial^2\psi}{\partial x_1^2}\Big)=0, \tag{14}$$

$$B_{44}\Big(\frac{\partial^3\psi}{\partial x_3^3}-\frac{\partial^3\psi}{\partial x_1^2\partial x_3}\Big)+(B_{11}-2B_{13}+B_{33})\frac{\partial^3\psi}{\partial x_1^2\partial x_3}$$
$$-\rho(1-\epsilon^2\nabla^2)\Big(\frac{\partial^3\psi}{\partial x_3\partial t^2}-\Omega^2\frac{\partial\psi}{\partial x_3}-2\Omega\frac{\partial^2\psi}{\partial x_1\partial t}\Big)=0. \tag{15}$$

From Eqs. (5) and (12), the decay condition becomes

$$\psi(x_1,x_3,t)\to 0 \text{ as } x_3\to+\infty. \tag{16}$$

For Rayleigh waves propagation in x_1-direction, the scalar function $\psi(x_1,x_3,t)$ is written as

$$\psi(x_1,x_3,t)=\phi(y)e^{ik(x_1-ct)},\ y=kx_3. \tag{17}$$

Substituting (17) in Eq. (6), a differential equation in ϕ is obtained as

$$[(1-e\Omega^*)D^4-\{\delta-2-\Omega^*(2e+V^{*2})\}D^2+\{1-\Omega^*(e+V^{*2})\}]\phi(y)=0, \tag{18}$$

where $V^{*2}=\rho c^2/B_{44}$ and the operator D denotes differentiation with respect to y.

With the help of Eq. (17), the boundary conditions (14) and (15) are expressed as

$$(D^2+1)\phi(0)=0, \tag{19}$$

$$[(1-e\Omega^*)D^3-2e\Omega_0D^2+\{1-\delta+\Omega^*(e+V^{*2})\}D+2\Omega_0(e+V^{*2})]\phi(0)=0. \tag{20}$$

From Eqs. (16) and (17), it follows that

$$\phi(x_3)\to 0 \text{ as } x_3\to+\infty. \tag{21}$$

The general solution $\phi(y)$ of Eq. (18) satisfying the decay condition (21) is expressed as

$$\phi(y)=Ae^{-m_1y}+Be^{-m_2y}, \tag{22}$$

where A and B are constants and m_1 and m_2 are solutions of

$$(1-e\Omega^*)m^4-\{\delta-2-\Omega^*(2e+V^{*2})\}m^2+\{1-\Omega^*(e+V^{*2})\}=0, \tag{23}$$

with positive real parts, i.e. $Re(m_k)>0$ $(k=1,2)$. From the latter, it follows that

$$m_1^2+m_2^2=\frac{\delta-2-\Omega^*(2e+V^{*2})}{1-e\Omega^*}, \tag{24}$$

$$m_1^2m_2^2=\frac{1-\Omega^*(e+V^{*2})}{1-e\Omega^*}. \tag{25}$$

The necessary condition for a Rayleigh wave to exist in the present model is $m_1^2 m_2^2 > 0$, which implies that

$$0 < V^{*2} < \frac{1}{\Omega^*} - e,\ e\Omega^* < 1. \tag{26}$$

Substituting the solution (22) in the boundary conditions (19) and (20), a homogeneous system of two equations in two unknowns A and B is obtained as

$$(m_1^2 + 1)A + (m_2^2 + 1)B = 0, \tag{27}$$

$$(a_1 m_1^3 + a_2 m_1^2 + a_3 m_1 + a_4)A + (a_1 m_2^3 + a_2 m_2^2 + a_3 m_2 + a_4)B = 0, \tag{28}$$

where $a_1 = e\Omega^* - 1,\ a_2 = -2e\Omega_0, a_3 = \delta - 1 - \Omega^*(e + V^{*2}),\ a_4 = 2\Omega_0(e + V^{*2})$.

For a non-trivial solution of above system of equations, the determinant of the coefficients of A and B in Eqs. (27) and (28) vanishes. After leaving the non-zero factor $(m_2 - m_1)$, we obtain the secular equation of Rayleigh wave as

$$a_1(m_1^2 + m_2^2 + m_1^2 m_2^2 + m_1 m_2) + (a_2 - a_4)(m_1 + m_2) + a_3(1 - m_1 m_2) = 0. \tag{29}$$

Eq. (29) is required dimensionless secular equation governing the speed of Rayleigh-type surface wave in an incompressible, rotating, transversely isotropic, nonlocal elastic half-space whose surface is subjected to the traction free boundary conditions.

5. LIMITING CASES

5.1. Nonlocal transversely isotropic elastic solid

In absence of rotation i.e. for $(\Omega \to 0)$, the rotation parameters $\Omega_0 \to 0$ and $\Omega^* \to 1$. Then, the secular equation (29) reduces to an equation with $m_1^2 + m_2^2 = (\delta - 2 - 2e - V^{*2})/(1 - e)$, $m_1^2 m_2^2 = (1 - e - V^{*2})/(1 - e)$, $a_1 = e - 1$, $a_3 = \delta - 1 - e - V^{*2}$, $a_2 = a_4 = 0$.

5.2. Local rotating transversely isotropic elastic solid

In absence of nonlocality $(\epsilon \to 0)$, the non-dimensional nonlocality parameter $e \to 0$. Then, the secular equation (29) reduces to an equation with $m_1^2 + m_2^2 = \delta - 2 - \Omega^* V^{*2}$, $m_1^2 m_2^2 = 1 - \Omega^* V^2$, $a_1 = -1$, $a_2 = 0$, $a_3 = \delta - 1 - \Omega^* V^{*2}$ $a_4 = 2\Omega_0 V^{*2}$.

5.3. Local transversely isotropic elastic solid

In absence of rotation $(\Omega \to 0)$ and nonlocality $(\epsilon \to 0)$, the parameters $\Omega_0 \to 0$, $\Omega^* \to 1$ and $e \to 0$. Then, the secular equation (29) reduces to an equation with $m_1^2 + m_2^2 = \delta - 2 - V^{*2}$, $m_1^2 m_2^2 = 1 - V^{*2}$, $a_1 = -1$, $a_3 = \delta - 1 - V^{*2}$, $a_2 = a_4 = 0$. Using the above relations, the secular equation (29) becomes

$$V^{*2} - (\delta - V^{*2})\sqrt{1 - V^{*2}} = 0, \tag{30}$$

which is analogous to the secular equation derived by Ogden and Vinh [53] for an incompressible orthotropic material.

6. NUMERICAL RESULTS AND DISCUSSION

Using velocity equation (9), the dependence of non-dimensional speed V of plane waves on the angle of propagation θ, rotation-frequency ratio Ω_0, non-dimensional material constant (anisotropy parameter) δ and non-dimensional nonlocal or small scale parameter e is illustrated graphically in Figs. 2 to 5.

In Fig. 2, the non-dimensional speed V of plane wave is plotted against the anisotropy parameter δ for $\theta = 45^\circ$, $\Omega_0 = 2$ and $e = 0, 0.05$ and 0.1. For $\theta = 45^\circ$, the inequality (10) reduces to the following inequality

$$\delta > 4e(1 + {\Omega_0}^2). \tag{31}$$

Using this inequality, the feasible ranges of δ in which the plane wave exists can be determined when other parameters e and Ω_0 are fixed. For $e = 0, 0.05$ and 0.1, the feasible ranges of δ are found as $(0, \infty)$, $(1, \infty)$ and $(2, \infty)$, respectively, when $\Omega_0 = 2$. For each value of e, the speed increases logarithmically in the respective feasible range of anisotropy parameter δ. The speed at each value of δ remains always higher in absence of small scale parameter. The nonlocality or small scale effect on the speed reduces at higher values of δ. For $e = 0, 0.05$ and 0.1, the speed at $\delta = 4$ in Fig. 2 correspond to the isotropic case.

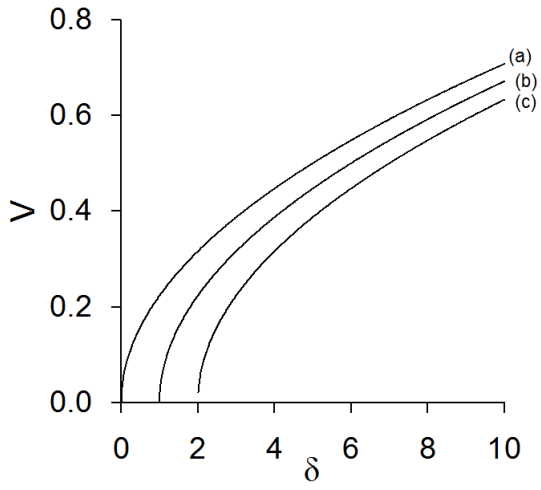

Fig. 2. Variations of non-dimensional speed V of plane wave against the non-dimensional anisotropy material parameter δ, when $\theta = 45^\circ$, $\Omega_0 = 2$ and for (a) $e = 0$ (b) $e = 0.05$ (c) $e = 0.1$

For $e = 0.05$, $\Omega_0 = 2$ and $\delta = 2, 4$ and 6, the non-dimensional speed V of plane wave is illustrated graphically in Fig. 3(i) against the propagation angle θ varying from 0° to 90°. For $\delta = 2$, the speed first decreases monotonically in range $0^\circ \leq \theta \leq 45^\circ$ and thereafter it increases monotonically for the remaining range of the propagation angle. For $\delta = 6$, the speed variation against θ is found to be opposite to that for $\delta = 2$. For $\delta = 4$ (isotropic case), the speed is independent of propagation angle θ. Comparing the

speed variations for different values of δ in Fig. 3(i) shows the effect of anisotropy on the plane wave speed at each angle θ. For angles $\theta_0 = 0^\circ$ and $\theta_0 = 90^\circ$, there is no anisotropy effect on the wave speed. The anisotropy effect is found maximum at angle $\theta = 45^\circ$. The non-dimensional speed V of plane wave is also plotted in Fig. 3(ii) against the propagation angle θ for $\delta = 6$, $\Omega_0 = 2$ and $e = 0, 0.05$ and 0.1. The small scale or nonlocality effect on the wave speed is observed at each angle of propagation and the speed remains always higher in absence of nonlocal parameter.

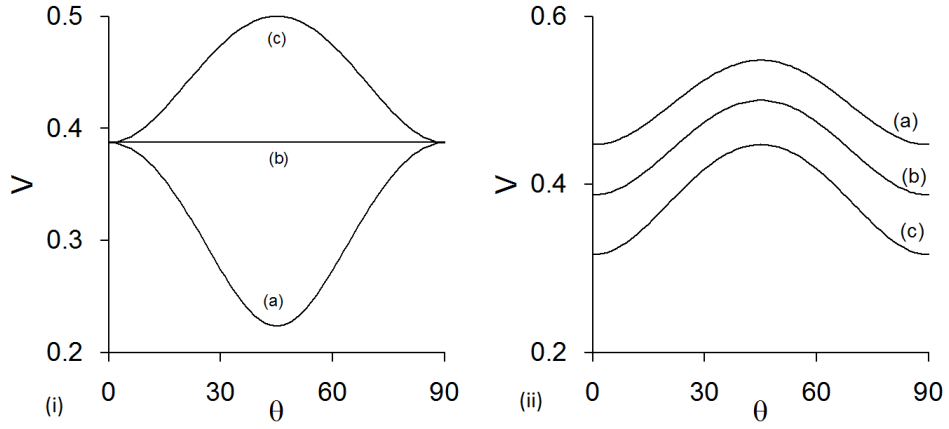

Fig. 3. Variations of non-dimensional speed V of plane wave against the angle of propagation θ when $\Omega_0 = 2$; (i) is plotted for $e = 0.05$ and for (a) $\delta = 2$ (b) $\delta = 4$ (c) $\delta = 6$; (ii) is plotted for $\delta = 6$ and for (a) $e = 0$ (b) $e = 0.05$ (c) $e = 0.1$

In Fig. 4(i), the non-dimensional speed V of plane wave is also plotted against the rotation parameter Ω_0 when $\theta = 45^\circ$, $\delta = 6$ and $e = 0, 0.05$ and 0.1. The feasible ranges

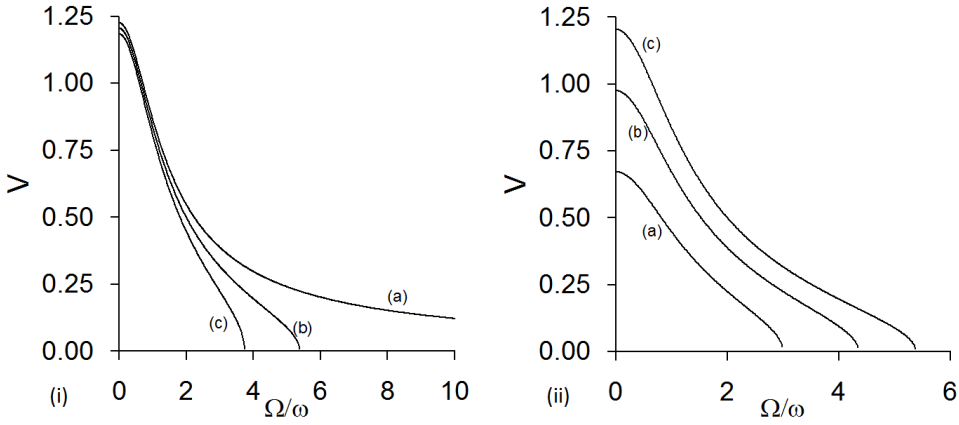

Fig. 4. Variations of non-dimensional speed V of plane wave against the rotation rate $\Omega_0(\Omega/\omega)$, when $\theta = 45^\circ$; (i) is plotted for $\delta = 6$ and for (a) $e = 0$ (b) $e = 0.05$ (c) $e = 0.1$; (ii) is plotted for $e = 0.05$ and for (a) $\delta = 2$ (b) $\delta = 4$ (c) $\delta = 6$

of rotation parameter Ω_0 for existence of plane wave are determined by using inequality (31). For $e = 0, 0.05$ and 0.1, the feasible ranges of Ω_0 are determined as $(-\infty, \infty)$, $(-\sqrt{29}, \sqrt{29})$ and $(-\sqrt{14}, \sqrt{14})$, respectively, when $\delta = 6$. For $e \geq 1.5$, the feasible range of Ω_0 for existence of plane wave can not be determined. For each value of e, the speed decreases monotonically in the positive feasible range of rotation parameter Ω_0. Comparing the speed variations for different e in Fig. 4(i) shows the small scale effect on the wave speed at different values of Ω_0. In Fig. 4(ii), the non-dimensional speed V of plane wave is illustrated graphically against the rotation parameter Ω_0 when $e = 0.05$, $\theta = 45^\circ$ and $\delta = 2, 4$ and 6. The feasible ranges of Ω_0 for $\delta = 2, 4$ and 6 are determined as $(-\sqrt{3}, \sqrt{3})$, $(-\sqrt{19}, \sqrt{19})$ and $(-\sqrt{29}, \sqrt{29})$, respectively, when $e = 0.05$. Comparing the speed variations for different values of δ in Fig. 4(ii) shows the anisotropy effect on the wave speed at different values of Ω_0.

In Fig. 5(i), the non-dimensional speed V of plane wave is illustrated graphically against the nonlocality parameter e when $\theta_0 = 45^\circ$, $\Omega_0 = 5$ and $\delta = 2, 4$ and 6. The feasible ranges of nonlocal parameter e for $\delta = 2, 4$ and 6 are determined as $[0, 1/52)$, $[0, 1/26)$ and $[0, 3/52)$, respectively, when $\Omega_0 = 5$. Therefore, the range of nonlocal parameter e expands as δ increases when Ω_0 is fixed. For each value of δ, the speed decreases at an increasing rate in the respective feasible range of nonlocal parameter e. The comparison of speed variations in Fig. 5(i) for different values of δ shows the anisotropy effect on wave speed at different values of e. Similar speed variations are also obtained in Fig. 5(ii) against nonlocality parameter e for different values of Ω_0 when $\theta_0 = 45^\circ$ and $\delta = 2$. For $\Omega_0 = 0, 1$ and 2, the feasible ranges of nonlocal parameter e are determined as $[0, 0.5)$, $[0, 0.25)$ and $[0, 0.1)$, respectively, when $\delta = 2$. Therefore, the range of nonlocal parameter e for existence of plane wave diminishes as Ω_0 increases. For each value of Ω_0, the speed also decreases at an increasing rate in the respective feasible range of nonlocal parameter e. The comparison of speed variations in Fig. 5(ii) for different values of Ω_0 shows the rotational effect on the wave speed at different values of e.

Using the secular equation (29), the dependence of non-dimensional speed of Rayleigh surface wave on rotation-frequency ratio Ω_0, non-dimensional material constant (anisotropy parameter) δ and non-dimensional nonlocality parameter e is shown graphically in Figs. 6 to 8.

In Fig. 6(i), the speed V^* of Rayleigh wave is plotted against δ for different values of nonlocal parameter e when $\Omega_0 = 4$. For each value of e, the speed increases logarithmically in respective feasible range of anisotropy parameter δ. The comparison of speed variations in Fig. 6(i) for different e shows the small scale effect on wave speed at different values of δ and the effect diminishes at larger values of δ. Fig. 6(ii) shows the rotational effect on wave speed at different values of δ and this effect becomes more prominent at larger values of δ.

For given value of δ, the small scale effect on Rayleigh wave speed V^* is illustrated graphically in Fig. 7(i) at different values rotation parameter Ω_0. In Fig. 7(ii), the anisotropy effect on wave speed is shown graphically at different rotation parameter Ω_0 when $e = 0.02$.

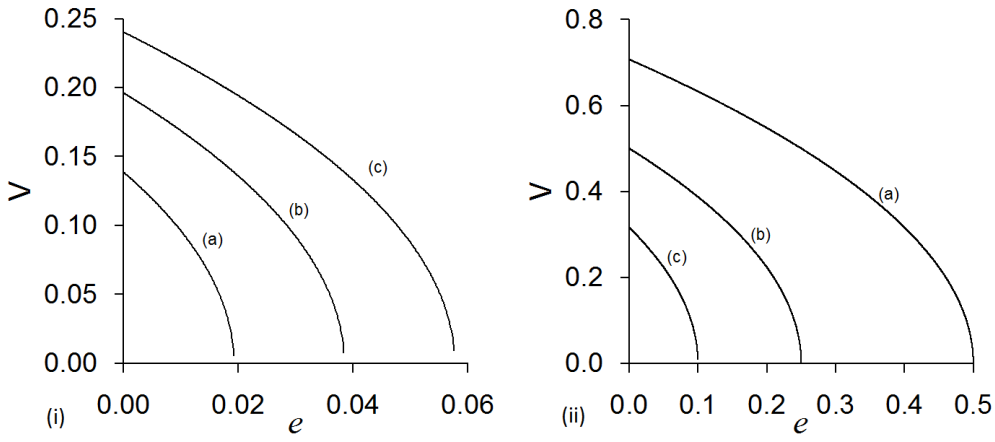

Fig. 5. Variations of non-dimensional speed V of plane wave against the non-dimensional nonlocality parameter e, when $\theta = 45^{\circ}$; (i) is plotted for $\Omega_0 = 5$ and for (a) $\delta = 2$ (b) $\delta = 4$ (c) $\delta = 6$; (ii) is plotted for $\delta = 2$ and for (a) $\Omega_0 = 0$ (b) $\Omega_0 = 1$ (c) $\Omega_0 = 2$

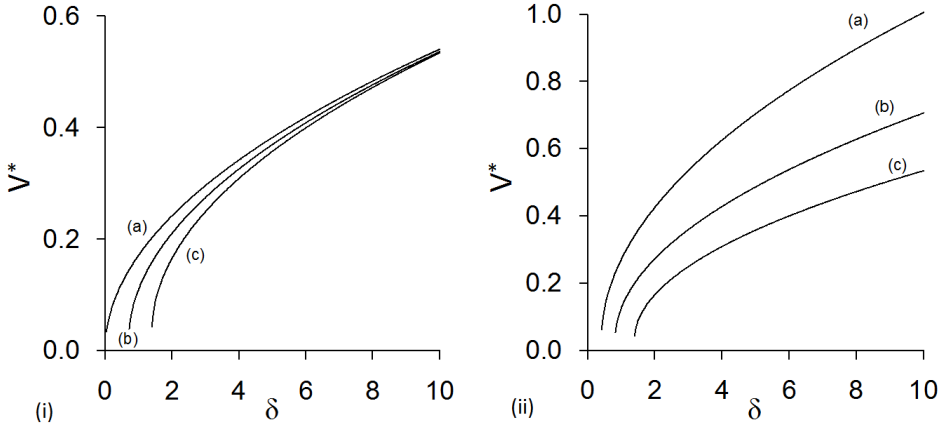

Fig. 6. Variations of non-dimensional speed V^* of Rayleigh wave against the non-dimensional constant δ; (i) is plotted for $\Omega_0 = 4$ and for (a) $e = 0$ (b) $e = 0.01$ (c) $e = 0.02$; (ii) is plotted for $e = 0.02$ and for (a) $\Omega_0 = 2$ (b) $\Omega_0 = 3$ (c) $\Omega_0 = 4$

The non-dimensional speed V^* of Rayleigh wave is also shown graphically against nonlocal parameter e in Fig. 8(i) for different values of δ. For each value of δ, the speed decreases at an increasing rate in the respective feasible range of nonlocal parameter e. The comparison of speed variations in figure 8(i) shows the anisotropy effect at a given value of e. Fig. 8(ii) shows the rotational effect on Rayleigh wave speed at a given nonlocal parameter. The range of nonlocal parameter e for existence of Rayleigh wave diminishes as Ω_0 increases.

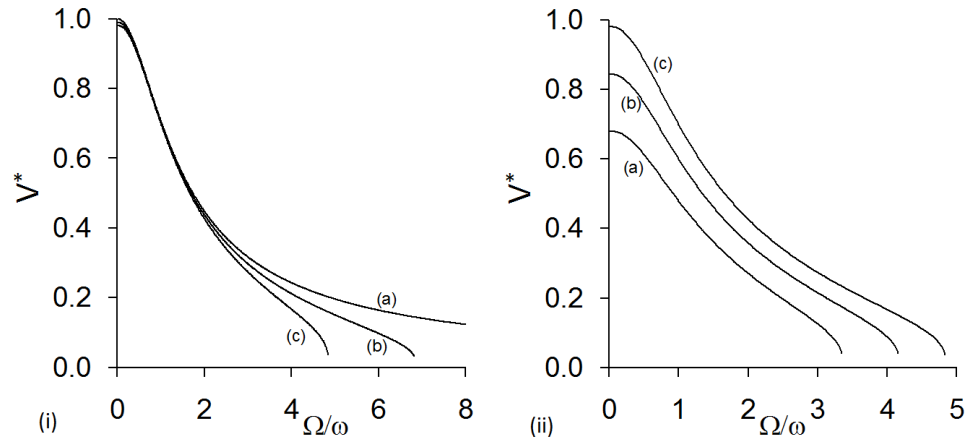

Fig. 7. Variations of non-dimensional speed V^* of Rayleigh wave against the rotation rate Ω_0; (i) is plotted for $\delta = 2$ and for (a) $e = 0$ (b) $e = 0.01$ (c) $e = 0.02$; (ii) is plotted for (a) $\delta = 1$ (b) $\delta = 1.5$ (c) $\delta = 2$

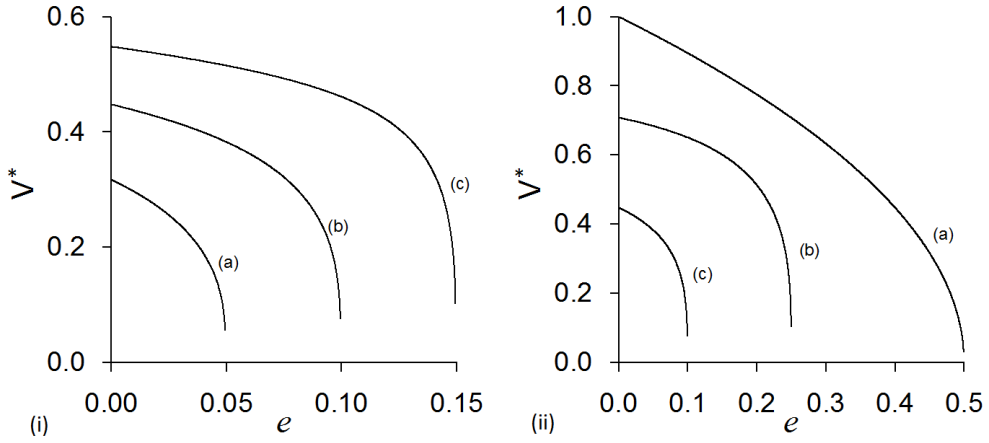

Fig. 8. Variations of non-dimensional speed V^* of Rayleigh wave against the non-dimensional nonlocality parameter e; (i) is plotted for $\Omega_0 = 2$ and for (a) $\delta = 1$ (b) $\delta = 2$ (c) $\delta = 3$; (ii) is plotted for $\delta = 2$ and for (a) $\Omega_0 = 0$(b) $\Omega_0 = 1$ (c) $\Omega_0 = 2$

7. CONCLUSIONS

A rotating and transversely isotropic half-space of an incompressible linearly nonlocal elastic material is considered for the propagation of plane wave and Rayleigh surface wave. Dispersive relations for plane wave and Rayleigh surface wave are derived. For different combinations of nonlocal parameter e, anisotropy parameter δ and rotation parameter Ω_0 which satisfy the inequalities (10) and (26), the speeds of plane wave and Rayleigh surface wave are computed and illustrated graphically. The graphical illustrations provide an interesting and new information on the behaviour of plane wave and

Rayleigh wave speeds in presence of nonlocality. Some important physical meanings from the theory and numerical simulations are derived as:

1. For all values of δ except $\delta = 4$ (isotropic case), the speed of plane wave varies with the propagation angle. The effect of anisotropy (transverse isotropy) on wave speed is observed maximum at $\theta = 45^\circ$ and minimum at angles $\theta = 0^\circ$ and 90°. The small scale effect on the wave speed is observed at each angle of propagation and the speed remains always higher in absence of nonlocal parameter.

2. Using inequalities (10) and (26), the ranges of anisotropy parameter δ or nonlocal parameter e or rotation parameter Ω_0 for existence of plane wave and Rayleigh wave can be estimated when values of other parameters are given.

3. The range of nonlocal parameter e for existence of plane wave or Rayleigh surface wave as estimated from the present numerical results is found in agreement with those proposed by Eringen [1,3,4].

4. The speeds of both plane wave and Rayleigh surface wave increase logarithmically in respective range of anisotropy material parameter δ for given values of nonlocal parameter e and rotation parameter Ω_0.

5. The speeds of both plane wave and Rayleigh surface wave decrease at increasing rate in the respective range of nonlocal parameter e for given values of δ and Ω_0.

6. The speeds of both plane wave and Rayleigh surface wave decrease monotonically in respective range of rotation parameter Ω_0 for given values of δ and e.

Therefore, the nonlocal elasticity theory predict the wave propagation phenomenon more accurately as compared to classical theory. The present theoretical and numerical results may help in predicting the behaviour of nanostructures which include the materials with dislocation, fractures, cracks, discontinuities and singularities.

REFERENCES

[1] A. C. Eringen. *Nonlocal continuum field theories*. Springer Verlag, New York, (2001).

[2] G. Z. Voyiadjis. *Handbook of nonlocal continuum mechanics for materials and structures*. Springer-Nature, Switzerland, (2019).

[3] A. C. Eringen. Linear theory of nonlocal elasticity and dispersion of plane waves. *International Journal of Engineering Science*, **10**, (1972), pp. 425–435. https://doi.org/10.1016/0020-7225(72)90050-x.

[4] A. C. Eringen. On differential equations of nonlocal elasticity and solutions of screw dislocation and surface waves. *Journal of Applied Physics*, **54**, (1983), pp. 4703–4710. https://doi.org/10.1063/1.332803.

[5] J. Peddieson, G. R. Buchanan, and R. P. McNitt. Application of nonlocal continuum models to nanotechnology. *International Journal of Engineering Science*, **41**, (2003), pp. 305–312. https://doi.org/10.1016/s0020-7225(02)00210-0.

[6] L. J. Sudak. Column buckling of multiwalled carbon nanotubes using nonlocal continuum mechanics. *Journal of Applied Physics*, **94**, (2003), pp. 7281–7287. https://doi.org/10.1063/1.1625437.

[7] Y. Q. Zhang, G. R. Liu, and J. S. Wang. Small-scale effects on buckling of multiwalled carbon nanotubes under axial compression. *Physical Review B*, **70**, (2004). https://doi.org/10.1103/physrevb.70.205430.

[8] A. Sears and R. C. Batra. Macroscopic properties of carbon nanotubes from molecular-mechanics simulations. *Physical Review B*, **69**, (2004). https://doi.org/10.1103/physrevb.69.235406.
[9] Q. Wang. Wave propagation in carbon nanotubes via nonlocal continuum mechanics. *Journal of Applied Physics*, **98**, (2005). https://doi.org/10.1063/1.2141648.
[10] L. Wang and H. Hu. Flexural wave propagation in single-walled carbon nanotubes. *Physical Review B*, **71**, (2005). https://doi.org/10.1103/physrevb.71.195412.
[11] G. Q. Xie, X. Han, and S. Y. Long. Effect of small size on dispersion characteristics of wave in carbon nanotubes. *International Journal of Solids and Structures*, **44**, (2007), pp. 1242–1255. https://doi.org/10.1016/j.ijsolstr.2006.06.019.
[12] Q. Wang and C. M. Wang. The constitutive relation and small scale parameter of nonlocal continuum mechanics for modelling carbon nanotubes. *Nanotechnology*, **18**, (2007). https://doi.org/10.1088/0957-4484/18/7/075702.
[13] A. Tounsi, H. Heireche, H. M. Berrabah, A. Benzair, and L. Boumia. Effect of small size on wave propagation in double-walled carbon nanotubes under temperature field. *Journal of Applied Physics*, **104**, (2008). https://doi.org/10.1063/1.3018330.
[14] B. Arash and R. Ansari. Evaluation of nonlocal parameter in the vibrations of single-walled carbon nanotubes with initial strain. *Physica E: Low-dimensional Systems and Nanostructures*, **42**, (2010), pp. 2058–2064. https://doi.org/10.1016/j.physe.2010.03.028.
[15] Y. Liang and Q. Han. Prediction of nonlocal scale parameter for carbon nanotubes. *Science China Physics, Mechanics and Astronomy*, **55**, (2012), pp. 1670–1678. https://doi.org/10.1007/s11433-012-4826-2.
[16] E. Ghavanloo and S. A. Fazelzadeh. Evaluation of nonlocal parameter for single-walled carbon nanotubes with arbitrary chirality. *Meccanica*, **51**, (2015), pp. 41–54. https://doi.org/10.1007/s11012-015-0195-z.
[17] S. Hemadi, S. E. Habibi, and P. Malekzadeh. Physically consistent nonlocal kernels for predicting vibrational characteristics of single walled carbon nanotubes. *Materials Today Communications*, **17**, (2018), pp. 322–331. https://doi.org/10.1016/j.mtcomm.2018.09.020.
[18] M. Tuna and M. Kırca. Unification of Eringen's nonlocal parameter through an optimization-based approach. *Mechanics of Advanced Materials and Structures*, **28**, (2019), pp. 839–848. https://doi.org/10.1080/15376494.2019.1601312.
[19] R. Ansari, S. Sahmani, and B. Arash. Nonlocal plate model for free vibrations of single-layered graphene sheets. *Physics Letters A*, **375**, (2010), pp. 53–62. https://doi.org/10.1016/j.physleta.2010.10.028.
[20] L. Y. Huang, Q. Han, and Y. J. Liang. Calibration of nonlocal scale effect parameter for bending single-layered graphene sheet under molecular dynamics. *Nano*, **07**, (2012). https://doi.org/10.1142/s1793292012500336.
[21] S. H. Madani, M. H. Sabour, and M. Fadaee. Molecular dynamics simulation of vibrational behavior of annular graphene sheet: Identification of nonlocal parameter. *Journal of Molecular Graphics and Modelling*, **79**, (2018), pp. 264–272. https://doi.org/10.1016/j.jmgm.2017.11.008.
[22] S. K. Jalali. Does vibration amplitude influence the evaluation of nonlocal small scale parameter of single layered graphene sheets? *Mechanics of Advanced Materials and Structures*, **27**, (2018), pp. 493–504. https://doi.org/10.1080/15376494.2018.1482035.
[23] B. Arash and Q. Wang. A review on the application of nonlocal elastic models in modeling of carbon nanotubes and graphenes. *Computational Materials Science*, **51**, (2012), pp. 303–313. https://doi.org/10.1016/j.commatsci.2011.07.040.

[24] M. N. L. Narasimhan and B. M. McCay. Dispersion of surface waves in nonlocal dielectric fluids. *Arch. Mech.*, **33**, (3), (1981), pp. 385–400.
[25] E. Inan and A. C. Eringen. Nonlocal theory of wave propagation in thermoelastic plates. *International Journal of Engineering Science*, **29**, (1991), pp. 831–843. https://doi.org/10.1016/0020-7225(91)90005-n.
[26] L.-L. Ke, Y.-S. Wang, and Z.-D. Wang. Nonlinear vibration of the piezoelectric nanobeams based on the nonlocal theory. *Composite Structures*, **94**, (2012), pp. 2038–2047. https://doi.org/10.1016/j.compstruct.2012.01.023.
[27] A. Sapora, P. Cornetti, and A. Carpinteri. Wave propagation in nonlocal elastic continua modelled by a fractional calculus approach. *Communications in Nonlinear Science and Numerical Simulation*, **18**, (2013), pp. 63–74. https://doi.org/10.1016/j.cnsns.2012.06.017.
[28] I. Roy, D. P. Acharya, and S. Acharya. Rayleigh wave in a rotating nonlocal magnetoelastic half-plane. *Journal of Theoretical and Applied Mechanics*, **45**, (2015), pp. 61–78. https://doi.org/10.1515/jtam-2015-0024.
[29] L. Tong, Y. Yu, W. Hu, Y. Shi, and C. Xu. On wave propagation characteristics in fluid saturated porous materials by a nonlocal Biot theory. *Journal of Sound and Vibration*, **379**, (2016), pp. 106–118. https://doi.org/10.1016/j.jsv.2016.05.042.
[30] D. Singh, G. Kaur, and S. K. Tomar. Waves in nonlocal elastic solid with voids. *Journal of Elasticity*, **128**, (2017), pp. 85–114. https://doi.org/10.1007/s10659-016-9618-x.
[31] G. Kaur, D. Singh, and S. K. Tomar. Rayleigh-type wave in a nonlocal elastic solid with voids. *European Journal of Mechanics - A/Solids*, **71**, (2018), pp. 134–150. https://doi.org/10.1016/j.euromechsol.2018.03.015.
[32] L.-H. Ma, L.-L. Ke, Y.-Z. Wang, and Y.-S. Wang. Wave propagation analysis of piezoelectric nanoplates based on the nonlocal theory. *International Journal of Structural Stability and Dynamics*, **18**, (2018). https://doi.org/10.1142/s0219455418500608.
[33] D.-J. Yan, A.-L. Chen, Y.-S. Wang, C. Zhang, and M. Golub. Propagation of guided elastic waves in nanoscale layered periodic piezoelectric composites. *European Journal of Mechanics - A/Solids*, **66**, (2017), pp. 158–167. https://doi.org/10.1016/j.euromechsol.2017.07.003.
[34] D. X. Tung. Dispersion equation of Rayleigh waves in transversely isotropic nonlocal piezoelastic solids half-space. *Vietnam Journal of Mechanics*, **41**, (2019), pp. 363–371. https://doi.org/10.15625/0866-7136/14621.
[35] B. Singh. Rayleigh-type surface waves in a nonlocal thermoelastic solid half space with voids. *Waves in Random and Complex Media*, (2020), pp. 1–12. https://doi.org/10.1080/17455030.2020.1721612.
[36] L. Rayleigh. On waves propagated along the plane surface of an elastic solid. *Proceedings of the London Mathematical Society*, **s1-17**, (1885), pp. 4–11. https://doi.org/10.1112/plms/s1-17.1.4.
[37] R. M. White. Acoustic sensors for physical, chemical and biochemical applications. In *Proceedings of IEEE International Frequency Control Symposium*, (1998), pp. 587–594.
[38] H. F. Tiersten, D. S. Stevens, and P. K. Das. Acoustic surface wave accelerometer and rotation rate sensor. In *Proceedings of IEEE Ultrasonics Symposium*, (1980), pp. 692–695.
[39] H. F. Tiersten, D. S. Stevens, and P. K. Das. Circulating flexural wave rotation rate sensor. In *Proceedings of IEEE Ultrasonics Symposium*, (1981), pp. 163–166.
[40] T. Wren and J. S. Burdess. Surface waves perturbed by rotation. *Journal of Applied Mechanics*, **54**, (1987), pp. 464–466. https://doi.org/10.1115/1.3173043.
[41] M. Schoenberg and D. Censor. Elastic waves in rotating media. *Quarterly of Applied Mathematics*, **31**, (1), (1973), pp. 115–125.

[42] J.-L. Auriault. Body wave propagation in rotating elastic media. *Mechanics Research Communications*, **31**, (2004), pp. 21–27. https://doi.org/10.1016/j.mechrescom.2003.07.002.
[43] N. S. Clarke and J. S. Burdess. A rotation rate sensor based upon a Rayleigh resonator. *Journal of Applied Mechanics*, **61**, (1994), pp. 139–143. https://doi.org/10.1115/1.2901388.
[44] N. S. Clarke and J. S. Burdess. Rayleigh waves on a rotating surface. *Journal of Applied Mechanics*, **61**, (1994), pp. 724–726. https://doi.org/10.1115/1.2901524.
[45] H. Fang, J. Yang, and Q. Jiang. Rotation-perturbed surface acoustic waves propagating in piezoelectric crystals. *International Journal of Solids and Structures*, **37**, (2000), pp. 4933–4947. https://doi.org/10.1016/s0020-7683(99)00198-5.
[46] M. Destrade. Rayleigh waves in anisotropic crystals rotating about the normal to a symmetry plane. *Journal of Applied Mechanics*, **71**, (2004), pp. 516–520. https://doi.org/10.1115/1.1756140.
[47] M. Destrade. Surface acoustic waves in rotating orthorhombic crystals. *Proceedings of the Royal Society of London. Series A: Mathematical, Physical and Engineering Sciences*, **460**, (2004), pp. 653–665. https://doi.org/10.1098/rspa.2003.1192.
[48] T. C. T. Ting. Surface waves in a rotating anisotropic elastic half-space. *Wave Motion*, **40**, (2004), pp. 329–346. https://doi.org/10.1016/j.wavemoti.2003.10.005.
[49] R. W. Ogden and B. Singh. The effect of rotation and initial stress on the propagation of waves in a transversely isotropic elastic solid. *Wave Motion*, **51**, (2014), pp. 1108–1126. https://doi.org/10.1016/j.wavemoti.2014.05.004.
[50] P. C. Vinh and T. T. T. Hue. Rayleigh waves with impedance boundary conditions in incompressible anisotropic half-spaces. *International Journal of Engineering Science*, **85**, (2014), pp. 175–185. https://doi.org/10.1016/j.ijengsci.2014.08.002.
[51] B. Singh and B. Kaur. Propagation of Rayleigh waves in an incompressible rotating orthotropic elastic solid half-space with impedance boundary conditions. *Journal of the Mechanical Behavior of Materials*, **26**, (2017), pp. 73–78. https://doi.org/10.1515/jmbm-2017-0016.
[52] B. Singh and B. Kaur. Rayleigh-type surface wave on a rotating orthotropic elastic half-space with impedance boundary conditions. *Journal of Vibration and Control*, **26**, (2020), pp. 1980–1987. https://doi.org/10.1177/1077546320909972.
[53] R. W. Ogden and P. C. Vinh. On Rayleigh waves in incompressible orthotropic elastic solids. *The Journal of the Acoustical Society of America*, **115**, (2004), pp. 530–533. https://doi.org/10.1121/1.1636464.